

Continual Face Forgery Detection via Historical Distribution Preserving

Ke Sun¹, Shen Chen², Taiping Yao², Xiaoshuai Sun¹, Shouhong Ding²,
Rongrong Ji^{*1}

^{1*}Key Laboratory of Multimedia Trusted Perception and Efficient Computing,
Ministry of Education of China, Xiamen University, China.

²Youtu Lab, Tencent, China.

Abstract

Face forgery techniques have advanced rapidly and pose serious security threats. Existing face forgery detection methods try to learn generalizable features, but they still fall short of practical application. Additionally, finetuning these methods on historical training data is resource-intensive in terms of time and storage. In this paper, we focus on a novel and challenging problem: Continual Face Forgery Detection (CFFD), which aims to efficiently learn from new forgery attacks without forgetting previous ones. Specifically, we propose a Historical Distribution Preserving (HDP) framework that reserves and preserves the distributions of historical faces. To achieve this, we use universal adversarial perturbation (UAP) to simulate historical forgery distribution, and knowledge distillation to maintain the distribution variation of real faces across different models. We also construct a new benchmark for CFFD with three evaluation protocols. Our extensive experiments on the benchmarks show that our method outperforms the state-of-the-art competitors.

Keywords: Face Forgery Detection, Continual Learning, Universal Adversarial Perturbation

1 Introduction

Over the past decades, face forgery methods have made significant strides, capturing the interest of both the academic and industrial realms [Thies et al. \(2015\)](#); [Rossler et al. \(2019\)](#); [Dolhansky et al. \(2020\)](#). These techniques have the prowess to create ultra-realistic forged faces, so convincing at times that they can easily deceive the human eye. This verisimilitude has far-reaching implications, giving rise to potential malicious misuse. Whether used in privacy infringements, identity fraud, or other deceptive practices, they pose severe societal challenges. Therefore, the need to engineer potent methods capable of differentiating real faces from

their forged counterparts has become increasingly paramount. Recently, many significant face forgery detection methods have been proposed to mine the subtle artifacts [Chen et al. \(2021\)](#); [Qian et al. \(2020\)](#); [Dolhansky et al. \(2020\)](#); [Dang et al. \(2020\)](#); [Afchar et al. \(2018\)](#); [Sun et al. \(2021\)](#); [Luo et al. \(2023, 2021\)](#) and achieved extraordinary performance under known forgery types. However, they all suffer from significant performance degradation when testing under new forgery attacks. Some methods have attempted to learn generalized representation [Li et al. \(2020\)](#); [Sun et al. \(2022\)](#); [Luo et al. \(2021\)](#); [Sun et al. \(2021\)](#); [?](#), but their performance on unknown attacks is still far from practical application. As face forgery

techniques continue to evolve, acquiring a comprehensive dataset of all forgery methods and their respective manipulation techniques becomes challenging, especially since such data is often accrued over time. Given this scenario, continually updating models to integrate both past and current data can be both time-consuming and storage-intensive. Relying solely on recent forgery data for model updates introduces the risk of catastrophic forgetting—a situation where the model forgets its previously learned patterns. These limitations present significant barriers to the practical deployment of face forgery detection systems in real-world scenarios.

To address this challenge, we introduce and tackle a novel and pressing problem: **Continual Face Forgery Detection** (CFFD) Li et al. (2023). CFFD evaluates the capacity of detectors to adapt to new attack techniques sequentially while retaining proficiency in recognizing earlier ones. As depicted in Fig.1, diverse training data are introduced across different stages. The goal of the model is to assimilate new information without discarding what it has previously learned. While certain existing continual learning methods might seem applicable to CFFD—such as regularization techniques Li and Hoiem (2017); Hou et al. (2019); Kirkpatrick et al. (2017), parameter-isolation strategies Rusu et al. (2016); Xu and Zhu (2018); Verma et al. (2021), and replay methods Rebuffi et al. (2017); Aljundi et al. (2019); Chaudhry et al. (2020)—these general approaches have not been expressly tailored for face forgery detection. This oversight often culminates in a performance that is less than ideal. To remedy this, we identify two distinct characteristics that differentiate CFFD from conventional continual learning: (1). Face forgery detection is inherently a binary classification task. It is mainly concerned with differentiating an array of fake faces, implying that features of real faces tend to exhibit more uniformity. (2). The differences between real and forged faces are subtle, putting the onus on the detection network to identify the discriminative differences effectively.

In this paper, we propose a novel Historical Distribution Preserving (HDP) framework that preserves the historical distributions of real and forged faces. The main challenge is *how to efficiently preserve historical forgery distribution and the discriminative differences from real faces?*

Motivated by the universal adversarial perturbation (UAP), which can be regarded as a *feature* that captures the main direction of image-space that affects the model decision Jetley et al. (2018); Zhang et al. (2020), we propose a new perspective of continual learning that uses the UAP as the discriminative feature of forged faces relative to real faces. Specifically, instead of storing redundant forged data, we only store a single UAP generated by the historical model. And when dealing with new forgery attacks, we combine the real faces and the UAP as the pseudo-forged faces to simulate historical forgery distribution. Such faces can not only reserve the discriminative feature of the forgery but also protect privacy from being violated. Feature-based knowledge distillation is further employed to maintain the distribution of real and pseudo-forged faces across different models to reduce the domain gap between each stage. The inherent uniformity of real-face features allows for easier maintenance of the real distribution and further ensures the restoration of historical distribution by the pseudo-forged samples.

Notably, our methodology demands minimal storage overhead and is seamlessly integrable with any classification-centric face forgery detection framework within the proposed CFFD paradigm. This bears significant ramifications for real-world implementations, where efficiency and adaptability are paramount. Extensive experiments on the CFFD benchmark show that our method not only outperforms state-of-the-art competitors but also exhibits exceptional resilience against continually evolving forgery techniques. In summary, our main contributions are as follows:

- We first exploit the Universal Adversarial Perturbation (UAP) into continual learning as the discriminative historical feature instead of storing samples.
- We propose a novel Historical Distribution Preserving (HDP) framework in the Continual Face Forgery Detection task to preserve the distributions of real and forgery faces and their discriminative distribution difference, thus mitigating catastrophic forgetting.
- We provide a benchmark with three evaluation protocols for the CFFD task. Extensive experiments and visualizations demonstrate the effectiveness of our method.

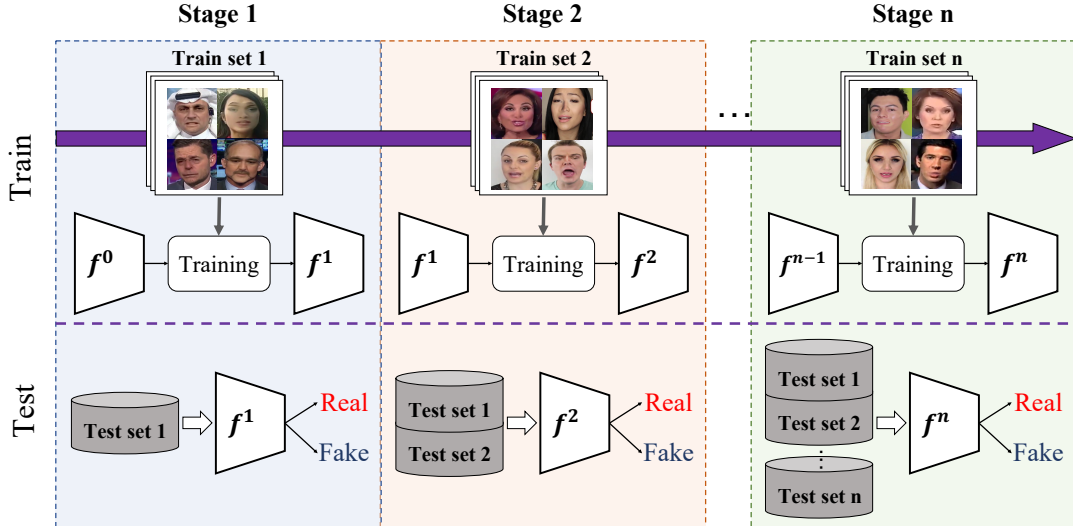


Fig. 1: Pipeline of the training and testing processes in the Continual Face Forgery Detection (CFFD) setting. (Best viewed in color.)

2 Related Work

2.1 Face Forgery Detection

Face forgery detection is mainly to identify whether the input face is forged or not. Early studies use hand-crafted features to seek the artifacts in forged faces Matern et al. (2019); Yang et al. (2019). Subsequently, deep learning-based works achieve better performance by extracting high-level features for classification. For example, some works Stehouwer et al. (2019); Zhao et al. (2021a) highlight the manipulated regions through attention mechanism, while others Chen et al. (2021); Zhao et al. (2021b) leverage the self-consistency of local regions as forged clues. Although these methods achieve extraordinary performance on seen forgery attacks, they suffer from significant performance degradation when testing under new forgery attacks. Subsequently, some methods have attempted to learn generalized representation. Face X-ray Li et al. (2020) conducts self-supervised learning driven by simulation of the blending traces. LTW Sun et al. (2021) uses meta-learning to reweight samples and provide gradient regularization. DCL Sun et al. (2022) controls the intra-class variance to preserve the transferability via contrastive learning. However, their performance on unseen attacks is

still far from practical application. With the continuous emergence of new forgery methods, it is difficult to obtain all forgery samples with various manipulation techniques at once. And performing finetune directly based on historical training data often requires much time and storage costs. To address these issues, We focus on a new yet practical face forgery detection task, named Continual Face Forgery Detection (CFFD) Li et al. (2023), which enables efficient learning to deal with continuous new attacks.

2.2 Continual Learning

Current continual learning methods can be taxonomized into three major categories Delange et al. (2021). 1) *Parameter isolation* methods intend to assign separate components for each task. These works typically require a task oracle Delange et al. (2021) that matches the corresponding dynamic layer to a special task, which increases the network complexity and is not conducive to practical deployment. 2) *Regularization-based* methods introduce an extra regularization term in the loss function to consolidate previous knowledge during training new tasks. Specifically, LwF Li and Hoiem (2017) uses the output of previous models as soft-label and treats the regularization term as knowledge distillation. EWC Kirkpatrick et al.

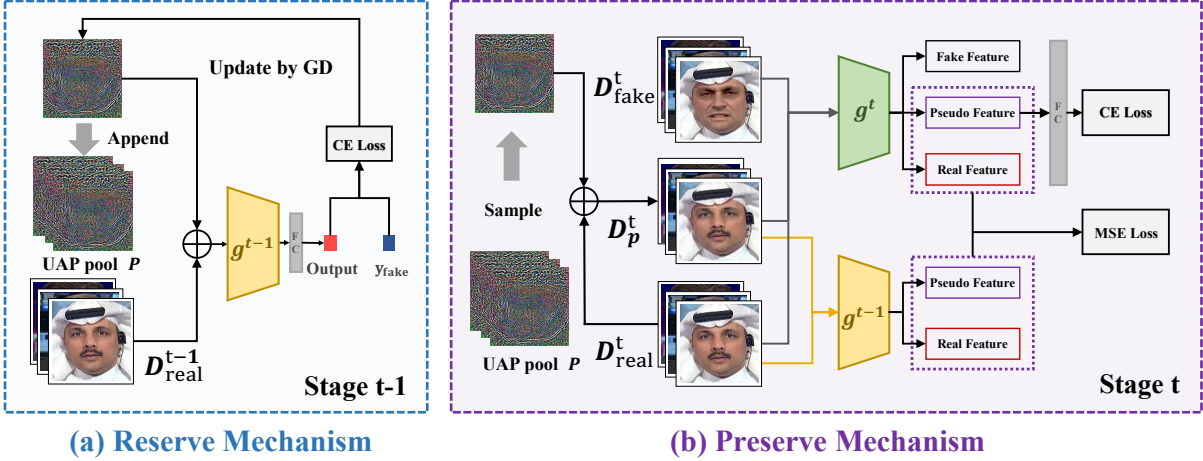


Fig. 2: Overview of the proposed Historical Distribution Preserving framework for CFFD task. Subfigure (a) elucidates the reservation mechanism and subfigure (b) details the preservation mechanism.

(2017) and MAS Aljundi et al. (2018) try to estimate a distribution over the model parameters. Other regularization-based methods estimate a distribution over the model parameters such as EWC Kirkpatrick et al. (2017) and MAS Aljundi et al. (2018). Though these approaches alleviate catastrophic forgetting to some extent, they may yield suboptimal performance when faced with challenging settings or complex datasets Wang et al. (2021). 3) *Replay-based* methods preserve the samples of previous tasks in a memory bank and replay them when learning the current task. The most classic method is iCaRL Rebuffi et al. (2017), which stores a subset of exemplars based on the distance of the class means center in the feature space. Recently, some works Buzzega et al. (2020); Chaudhry et al. (2020); Wu et al. (2019) combine the knowledge distillation regularization with a memory bank to further avoid overfitting. Although replay methods can alleviate catastrophic forgetting well, the performance is vulnerable to the size of buffers, and the extra memory bank may also bring data privacy leakage and storage burden. Differently, we propose a new perspective of continual learning that introduces the universal adversarial perturbation (UAP) to simulate historical distribution. Remarkably we store only one UAP generated by the historical model without any additional rehearsal buffers, while still achieving better performance than traditional replay methods.

2.3 Universal Adversarial Perturbation

Universal Adversarial Perturbation (UAP) Moosavi-Dezfooli et al. (2017) is a specially designed noise that can fool the deep learning model with high probability. Different from the per-instance adversarial examples Szegedy et al. (2013), UAP needs to compute only a single perturbation vector to fool all the images. Moosavi-Dezfooli et al. Moosavi-Dezfooli et al. (2017) first formulate and generate UAP via iterative deepfool Moosavi-Dezfooli et al. (2016). Meanwhile, the interpretability of UAP has drawn lots of attention in the computer vision community. Moosavi-Dezfooli et al. Moosavi-Dezfooli et al. (2018) theoretically proved that the existence of a low dimension subspace that captures the correlation between the decision boundary of the target model is the reason why UAP works Chaubey et al. (2020). Furthermore, Jetley et al. Jetley et al. (2018) reveals the consistency in model performance and robustness. Zhang et al. Zhang et al. (2020) demonstrate that the UAP themselves contains features independent of the images to attack. Inspired by their seminal analysis, our method utilizes UAP and the corresponding data to approximate the previous feature distribution and replay it when training the new task.

3 Method

3.1 Problem Definition

The goal of Continual Face Forgery Detection (CFFD) is to develop a unified detector from a sequence of face data encompassing different forgery types and domains. Formally, we denote the training data available at the t -th stage as $D^t = \{D_{\text{real}}^t, D_{\text{fake}}^t\}$, where D_{real}^t and D_{fake}^t represent the incoming real and forged faces, respectively. The face forgery detection model for the t -th stage, f^t , is trained exclusively from the dataset D^t . Data from the previous stages, $\{D^t\}_{t=1}^{t-1}$, are no longer accessible. This framework is motivated by two primary considerations: first, it sidesteps the storage overhead and the associated computational challenges posed by a vast archive of historical data; second, privacy constraints might make historical face data unavailable. For evaluation, the model f^t is tested against all previously identified forgery attacks, ensuring that its robustness and adaptability are rigorously assessed across a comprehensive range of scenarios.

3.2 Base Training

In this section, we outline the fundamental strategy for training the face forgery detection model. Practically, our proposed approach can be incorporated into any State-Of-The-Art (SOTA) classification-based method. For the sake of clarity, we employ the widely recognized binary classifier model [Dolhansky et al. \(2020\)](#), using cross-entropy loss to optimize the model on dataset D . This is expressed as:

$$L_{ce} = -\frac{1}{|D|} \sum_{(x,y) \in D} y \log(f(x)) + (1-y) \log(1-f(x)), \quad (1)$$

where $x \in \mathbb{R}^{\text{C} \times \text{H} \times \text{W}}$ and $y \in \{0, 1\}$ denote the images and their corresponding labels (real/fake) from the dataset D , respectively. At the t -th stage, if we employ cross-entropy loss directly on $D^t = \{D_{\text{real}}^t, D_{\text{fake}}^t\}$, the model f^t will recognize the forgery types it has been exposed to but will likely forget about earlier forgery techniques. Hence, the primary challenge of CFFD lies in preserving the historical forgery distribution and the discriminative differences between real and forgery faces.

3.3 Overall Framework

For continual face forgery detection, we introduce a Historical Distribution Preserving (HDP) framework. This framework tackles the challenge of catastrophic forgetting with two main components: the Reserve Mechanism and the Preserve Mechanism. The operational flow of the HDP is depicted in Fig.2. Within the Reserve Mechanism, we utilize the Universal Adversarial Perturbation (UAP) [Moosavi-Dezfooli et al. \(2017\)](#) as the discriminative feature distinguishing forged faces from real ones. Specifically, we generate the UAP from the proficiently trained model f^{t-1} , encapsulating the most discerning features of forgery attacks up to the $t-1$ stage and storing them in the UAP pool. Transitioning to a new attack at the t stage, we deploy the Preserve Mechanism. This strategy begins by melding real faces with the generated UAPs, simulating the distribution of forgery attacks from previous stages. Subsequently, this synthesized data is trained in tandem with the fresh dataset. Furthermore, we conduct feature-wise knowledge distillation between pseudo and real features across the current and the last step model to maintain the stability of the distribution in all stages.

3.4 Reserve Mechanism

The primary objective of this mechanism is to preserve the historical forgery distribution by a combination of Universal Adversarial Perturbation (UAP) and real data. As highlighted in prior studies [Zhang et al. \(2020\)](#); [Jetley et al. \(2018\)](#), UAP embodies a feature that consistently imparts directional perturbations across class boundaries, regardless of the diverse individual appearances. Furthermore, [Jetley et al. \(2018\)](#) elucidated the profound correlation between specific directions and class identity—essentially, the network discerns these directions as features inherently associated with class identities. Consequently, we employ UAP as a distinctive feature to differentiate forged faces from real ones, combining it with real faces to synthesize pseudo-forged samples. For a model f^{t-1} trained during the $t-1$ phase, which incorporates a feature extractor g^{t-1} , an FC layer, and real subset samples $x_{\text{real}}^{t-1} \in D_{\text{real}}^{t-1}$ labeled $y_{\text{real}} = 0$, our goal is to ascertain perturbation vectors $p^{t-1} \in \mathbb{R}^{\text{C} \times \text{H} \times \text{W}}$ capable of misleading the model into misclassifying real

images as fake. Analogous to Moosavi-Dezfooli et al. (2017), we target a vector p^{t-1} that conforms to:

$$\begin{aligned} \text{Pred}(f^{t-1}(x_{\text{real}}^{t-1} + p^{t-1})) &\neq y_{\text{real}} \\ \text{s.t. } \|p^{t-1}\|_{\infty} &\leq \epsilon, \end{aligned} \quad (2)$$

where Pred translates the logit to a prediction value (i.e., 0 for real and 1 for fake), and ϵ modulates the magnitude of the perturbation vector. We denote the pseudo-forged samples x_p^{t-1} as:

$$x_p^{t-1} = x_{\text{real}}^{t-1} + p^{t-1}. \quad (3)$$

Contrary to the native UAP approach Moosavi-Dezfooli et al. (2017) that deploys deep-fool Moosavi-Dezfooli et al. (2016) to ascertain perturbations defining the decision boundary, our strategy interprets UAP as a potent feature. Taking a cue from Zhang et al. (2020), we utilize the gradient descent technique to refine p^{t-1} by minimizing the entropy between pseudo-forged samples x_p^{t-1} and the fake label $y_{\text{fake}} = 1$. This process is encapsulated as:

$$p^{t-1} = p^{t-1} - \alpha * \text{sgn}(\nabla_{p^{t-1}} \log(f^{t-1}(x_p^{t-1}))), \quad (4)$$

where sgn represents the symbolic function, and α signifies the learning rate of p^{t-1} . The perturbation is reiterated until x_p^{t-1} transgresses the decision boundary. The algorithm concludes when the number of successfully modified prediction outcomes surpasses the predetermined threshold σ . Upon deriving the UAP p^{t-1} , we integrate it into the UAP pool P in anticipation of the rehearsal phase, which substantially minimizes computational strain and storage encumbrance.

3.5 Preserve Mechanism

Upon reversing the historical distribution, the subsequent step is to retain the forgery distribution by integrating them into the ongoing training process. Specifically, during the t -th stage of training, entropy optimization is employed for the pseudo-forged samples paired with their fake labels. This introduces a regularization term, ensuring the distribution of the pseudo-forged samples is duly preserved.

Algorithm 1 Historical Distribution Preserving

Input: Dataset $D = \{D_{\text{real}}^t, D_{\text{fake}}^t\}_{t=1}^T$, initial model f^0 , UAP pool P .

Init: $P \leftarrow \{\}$

```

1: for  $\{D_{\text{real}}^t, D_{\text{fake}}^t\} \in D$  do
2:   if  $t == 1$  then
3:     Optimize  $f^0$  with Eq.1 to obtain  $f^1$ .
4:   else
5:     Optimize  $f^{t-1}$  with Eq.8 to obtain  $f^t$ .
6:   end if
7:   Generate UAP  $p^t$  for model  $f^t$ .
8:   Append  $p^t$  into the  $P$ .
9: end for
10: Return model  $f^T$ 

```

During the training of model f^t with the dataset D^t , UAP from stages up to $t-1$, represented by $\{p^n\}_{n=1}^{t-1}$, is sequentially sampled from the UAP pool P before each training iteration. Following this, the pseudo-forged dataset D_p^n is produced via pixel-wise summation of p^n and D_{real}^t , expressed as $D_p^n = p^n + D_{\text{real}}^t$, associated with the label $y_{\text{fake}} = 1$. The entropy of D_p^n and the fake label y_{fake} is then computed as:

$$E^n = -\frac{1}{|D_p^n|} \sum_{x_p^n \in D_p^n} \log(f^t(x_p^n)). \quad (5)$$

To quantify the overall training entropy E^t at the t -th stage, one must consider the cumulative effect of various entropies E^n that have been sequentially sampled from the UAP pool. Thus, the overall training entropy is not just influenced by the current stage but is an accumulation of the influences from prior stages as well. This ensures that the distribution of forgery attacks from the previous stage is perpetuated. Nevertheless, given that parameters undergo dynamic optimization, the consistency of the pseudo-forged distribution might be compromised. Addressing this concern, we implement feature-wise knowledge distillation, utilizing the prior feature extractor g^{t-1} . This maintains distillation based on the pseudo-forged samples x_p^t , and is formalized as:

$$L_p^t = \frac{1}{|D_p^n|} \sum_{x_p \in D_p^n} \|g^t(x_p) - g^{t-1}(x_p)\|^2. \quad (6)$$

It’s noteworthy that in face forgery detection, the emphasis is predominantly on discerning forgery traces rather than differentiating between real and fake facial content. In practical applications, genuine images exhibit a relative homogeneity compared to their forged counterparts. Nonetheless, new forgery techniques can alter the real distribution, influencing the simulation of pseudo-forged samples. To counteract this, we emphasize maintaining the continuity of real distillation. Following the same paradigm as L_p , a single-set feature-based knowledge distillation is applied. Without any compromise to generality, let g^t be the feature extractor for the model f^t . Here, the previous feature extractor, g^{t-1} , is regarded as the teacher, utilizing the mean-squared function as the regularization term. This can be articulated as:

$$L_r^t = \sum_{x \in D_{real}^t} \|g^t(x) - g^{t-1}(x)\|^2. \quad (7)$$

By regularizing each training stage using the model from the preceding phase, the real sample distribution remains consistent, ensuring stability.

3.6 Loss Function

In summary, when new forgery attacks arise at the t stage, the overall loss function for our proposed method of preserving historical distribution is defined as the sum of the base training loss and the aforementioned distribution-preserving optimizations. This can be expressed as:

$$L^t = L_{ce}^t + E^t + \beta(L_r^t + L_p^t), \quad (8)$$

where β is a hyper-parameter that weighs the regularization terms. To offer a clearer understanding of our method, we provide the pseudo-code of the HDP in Alg 1.

4 Experiment

4.1 Experimental Setting

Datasets. We conduct experiments based on four challenging datasets: FaceForensics++ [Rossler et al. \(2019\)](#) (FFpp) is a widely-used dataset containing four different face synthesis methods, including two deep learning-based methods Deepfakes (DF) and NeuralTextures (NT) and two

graphics-based approaches Face2Face (FF) and FaceSwap (FS). Celeb-DF [Li et al. \(2020\)](#) is another Deepfake dataset that collects real source videos from Youtube and generates forgery videos using an improved DeepFake synthesis method, resulting in a higher quality of forgery samples. DFDC [Dolhansky et al. \(2020\)](#) is a large-scale dataset with various manipulated methods and backgrounds. Wild-Deepfake [Zi et al. \(2020\)](#) is a face forgery dataset where all videos are obtained from the internet, thus it has various synthesis methods, identities, and image qualities.

CFFD Benchmark. We introduce a novel CFFD benchmark that encompasses three protocols, each escalating in difficulty.

Protocol 1: This protocol comprises four fake subsets from FFpp. Though these subsets maintain consistency in context and individual identity, they vary in their manipulation types. The core objective of Protocol 1 is to emulate the continuous emergence of novel attack strategies.

Protocol 2: Diversifying the range, this protocol draws from four fake datasets, namely FFpp, Celeb-DF, Wild-Deepfake, and DFDC. When juxtaposed with Protocol 1, Protocol 2 exhibits a wider array of attack types and more pronounced domain gaps. The real samples in this protocol differ at each stage, which elevates its difficulty. This intricacy, combined with its expansive applicability, positions Protocol 2 as particularly challenging.

Protocol 3: Tailored to assess the ability to handle extended sequences of evolving real and fake imagery, this protocol unfolds across ten stages. It utilizes subsets from FFpp and evenly apportions the datasets from Celeb-DF, Wild-Deepfake, and DFDC. This layout accentuates the risk of catastrophic forgetting. Between the three protocols, Protocol 3 most accurately mirrors the complexities of real-world scenarios, typified by extended sequences and multi-domain data. For an in-depth exploration of the three protocols, please refer to the supplementary materials.

Evaluation Metrics. Our primary evaluation metrics encompass the accuracy score (ACC) and the area under the receiver operating characteristic curve (AUC). Both ACC and AUC are standard measures to evaluate the performance of classification models. While ACC measures the proportion of correctly classified instances out of the total instances, AUC provides an aggregate

Method	Buffer /Step	Deepfakes		Face2Face		FaceSwap		NeuralTextures		AVG		PRE	
		ACC	AUC	ACC	AUC	ACC	AUC	ACC	AUC	ACC	AUC	ACC	AUC
SFT	0	76.88	91.88	68.15	85.57	59.74	72.78	<u>95.53</u>	98.43	75.07	87.16	67.29	88.36
LwF	0	81.51	95.61	72.26	91.81	61.27	81.38	95.48	<u>98.28</u>	77.63	91.77	74.09	94.05
MAS	0	86.97	95.14	78.01	86.81	65.89	72.89	90.86	96.15	80.43	87.74	<u>83.76</u>	90.75
NCM	0	76.94	92.90	67.67	92.99	61.77	70.75	95.66	96.81	75.53	85.28	69.13	87.73
iCaRL	500	84.46	95.67	81.71	93.28	73.41	87.01	94.70	98.15	83.57	93.52	82.82	93.84
SCR	500	82.85	<u>96.75</u>	81.42	<u>94.79</u>	62.96	89.49	95.53	97.33	80.69	86.75	75.29	<u>95.27</u>
FReTAL	500	<u>86.95</u>	94.26	<u>88.55</u>	93.65	<u>88.50</u>	<u>94.85</u>	94.43	98.25	<u>89.53</u>	<u>95.25</u>	80.07	95.24
DER	500	78.41	87.82	73.32	82.63	71.80	74.24	88.91	93.14	77.86	84.45	80.50	89.10
DER++	500	81.20	94.10	74.93	88.90	70.15	76.20	90.23	97.40	79.12	88.64	80.60	89.09
Co2L	500	84.91	94.81	76.50	86.81	64.99	73.95	94.36	97.64	80.19	88.30	77.52	89.00
HDP	0	93.10	98.17	91.90	96.86	93.47	97.52	94.81	97.12	93.32	97.41	94.94	98.50
Joint	-	96.99	99.75	96.35	99.12	96.63	99.30	94.04	97.84	96.00	99.00	-	-

Table 1: Quantitative results on protocol1 in terms of ACC and AUC. We evaluate the last model on all the previous test sets. The buffer represents the memory bank budget save the previous images per stage.

measure of the model’s performance across all possible classification thresholds.

In the context of the CFFD benchmark, we employ two primary metrics:

AVG (Average Performance) represents the performance of the *last model* over each individual task. By evaluating the last model across the various tasks, we aim to understand how well the continually updated model performs on different challenges, especially the most recent ones. In mathematical terms, AVG calculates the mean of the performance metric (be it ACC or AUC) of the last model on each separate task.

PRE (Performance on Previous Tasks) is designed to gauge the model’s resilience against catastrophic forgetting. Catastrophic forgetting refers to the model’s tendency to overwrite previous knowledge when learning new information. PRE, therefore, calculates the average performance metric of the model on all previous tasks, relative to the current task. A high PRE score indicates that the model retains its proficiency on prior tasks even after being updated with new tasks, showcasing its resistance to catastrophic forgetting.

Implementation Details. To ensure a fair comparison, all comparative methods are aligned to the following settings, unless specified otherwise. We utilize the EfficientNet-b4 [Tan and Le \(2019\)](#), pre-trained on ImageNet [Deng et al. \(2009\)](#), as the backbone for our face forgery detection model. DSFD [Li et al. \(2019\)](#) serves as our face detector across all datasets. All input face images are resized to a resolution of 224×224 . For model

training, we employ the Adam optimizer. Key parameters are set as follows: weight decay is $1e - 5$, the learning rate is 0.001, and the batch size is fixed at 64. While generating the UAP, we adjust the norm of perturbation (ϵ) to 0.15, set α at 0.0001, and determine the successful threshold (σ) to be 0.8. The complete framework is realized using PyTorch and is run on a single NVIDIA A-100 GPU.

4.2 Quantitative Results

Comparing Methods. We benchmark our method against several state-of-the-art continual learning techniques: including 1) Sequence fine-tune (SFT): Directly fine-tune model on new task dataset without extra operation; 2) Learning without forgetting (LwF) [Li and Hoiem \(2017\)](#): A regularization-based technique that retains previous knowledge via knowledge distillation. 3) Memory Aware Synapses (MAS) [Aljundi et al. \(2018\)](#): Another regularization-based strategy that forms the regularization term using the previous model parameters and their corresponding importance weight. 4) Nearest Class Mean Classifier for real sample ((NCM*) [Zhang et al. \(2020\)](#)): This method adjusts the unified classifier to our setting, constraining the real cluster centers and using the NCM classifier in place of the softmax-fc layer. 5) iCaRL [Rebuffi et al. \(2017\)](#): A well-known replay method that chooses to best approximate class means in the feature space and stores them in a memory bank. 6) Supervised Contrastive Replay

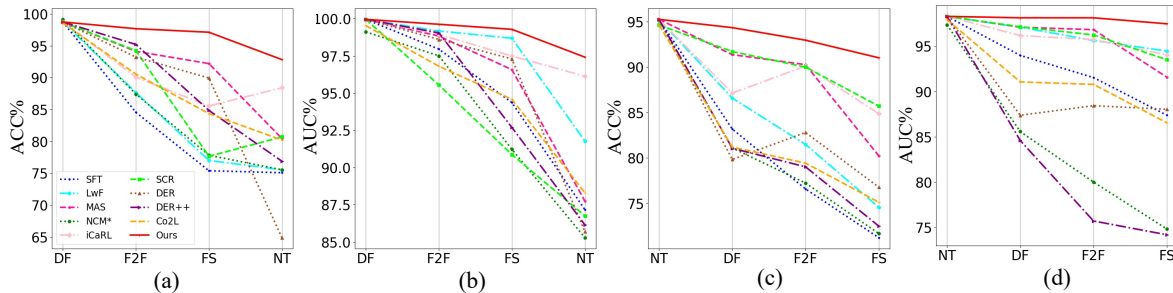


Fig. 3: Illustration of the non-forgetting evaluation of each stage on protocol 1. (a) and (b) show the trend of average AUC and ACC for the previous dataset during the training process for order 1, respectively. (c) and (d) represent the order2.

(SCR) [Mai et al. \(2021\)](#): A recent replay technique that merges supervised contrastive learning with the NCM classifier. 7) Continual Representation using Distillation (FReTAL) [Kim et al. \(2021\)](#): The first approach that considers continual learning settings within the face forgery detection task. 8) Dynamically Expandable Representation (DER) and DER++ [Yan et al. \(2021\)](#): A unique two-stage learning approach that employs dynamically expandable representation for more effective incremental concept modeling. 9) Contrastive Continual Learning (Co2L) [Cha et al. \(2021\)](#): This method learns representations through the contrastive learning objective and preserves these representations using a self-supervised distillation step. For all the replay methods mentioned above, we set the memory buffer size to hold 500 forgery images for each task.

Quantitative Results on Protocol1. Since sequence order is agnostic in continual learning, two orders are evaluated in protocol 1. *Order1* is represented by $DF \rightarrow F2F \rightarrow FS \rightarrow NT$ and *Order2* is $NT \rightarrow DF \rightarrow F2F \rightarrow FS$. The adjacent attack types in Order1 are more alike, in contrast to Order2, where the manipulation methods between stages are distinct. The results of *Order1* are shown in Tab. 1, while that of *Order2* are presented in the Appendix due to paper space limitations. In In Tab.1, it’s evident that our proposed approach significantly surpasses the competing methods in terms of both ACC and AUC metrics. Relative to the SFT, which grapples with pronounced catastrophic forgetting, our method sees approximately a 27% enhancement in the PRE

metric. This uplift primarily stems from the introduced historical distribution preservation strategy. Further, the performance of regularization-centric strategies, like LwF and MAS, is hampered by the pronounced domain gap between Celeb-DF and NeuralTextures — a challenge our method can adeptly navigate. Unlike existing replay strategies that demand large buffer sizes, our method requires storing only one UAP per task, giving us an advantage in preventing forgetting with minimal storage overhead.

To further show the ability to combat forgetting, we illustrate the average performance of the previous task and current task during each training process on *order1* and *order2*, respectively. As shown in Fig. 3 (a) and (b), our methods can achieve state-of-the-art results under different stages on both ACC and AUC. Fig. 3 (c), (d) summarizes the results on the *order2*. Similar to the *order1*, our method achieves the SOTA performance of AVG and PER compared with other methods on *order2*. Specifically, when facing the more difficult order, the ACC of AVG and PRE still obtain 20% and 25% improvement compared with SFT. The detailed results of Order2 are presented in the Appendix. The above results demonstrate the effectiveness and robustness of our approach to different task sequencing.

Quantitative Results on Protocol2. In Protocol 2, which is characterized by a substantial domain gap, the input order is set as $FFpp \rightarrow Celeb-DF \rightarrow WildDeepfake \rightarrow DFDC$.

As seen in Tab. 2, our method notably surpasses other comparative methods in terms of both ACC and AUC for AVG and PRE metrics. Specifically,

Method	Buffer /Step	FFpp		Celeb-DF		Wild-Deepfake		DFDC		AVG		PRE	
		ACC	AUC	ACC	AUC	ACC	AUC	ACC	AUC	ACC	AUC	ACC	AUC
SFT	0	85.02	93.88	81.75	90.17	72.59	83.27	<u>87.74</u>	<u>95.67</u>	81.77	90.82	79.92	89.38
LwF	0	87.08	96.64	83.82	90.69	73.77	84.85	87.12	94.84	82.94	91.75	82.93	92.84
MAS	0	85.45	97.16	81.17	89.29	76.91	81.03	87.03	90.10	81.86	91.64	82.22	92.00
NCM	0	85.83	93.44	83.76	90.22	77.01	83.72	86.56	93.76	83.29	90.28	80.38	90.14
iCaRL	500	85.50	95.62	85.07	92.77	74.87	84.49	87.81	95.46	83.38	92.08	84.21	93.15
SCR	500	86.90	96.46	<u>86.01</u>	92.99	76.71	85.59	88.19	95.63	84.45	92.66	83.30	93.97
FReTAL	500	<u>90.67</u>	<u>96.78</u>	85.62	<u>94.26</u>	76.58	86.34	87.12	95.52	84.99	93.22	83.70	93.43
DER++	500	87.89	94.40	84.92	91.05	73.58	85.48	87.29	95.35	83.42	91.57	83.35	93.77
Co2L	500	87.69	95.77	84.57	90.08	73.79	81.20	86.30	91.77	83.08	89.70	83.07	92.57
HDP	0	87.81	96.48	86.91	93.20	<u>78.03</u>	<u>87.21</u>	87.51	95.05	<u>85.63</u>	<u>93.23</u>	<u>86.99</u>	<u>94.09</u>
HDP	50	91.57	98.26	87.68	94.98	80.31	87.91	88.86	95.77	86.53	94.03	88.57	95.31
Joint	-	96.05	99.67	98.53	99.89	83.39	90.40	87.56	96.60	91.88	96.64	-	-

Table 2: Quantitative results on protocol2. We evaluate the last model on the test sets of all tasks in terms of ACC and AUC. The training order is FFpp \rightarrow Celeb-DF \rightarrow WildDeepfake \rightarrow DFDC. The buffer represents the memory bank budget save the previous images per stage. Underline indicate the sub-optimal results.

the ACC for PRE registers at 86.99%, marking a 7% enhancement from the baseline SFT. Our technique achieves state-of-the-art (SOTA) performance without any buffer, distinguishing it from other methods reliant on buffers. In contrast to buffer-based strategies like FReTAL, which reserves 500 images per stage, our method attains a 3% boost in the PRE metric without retaining any historical data. Additionally, when we augment our HDP to accommodate historical data with a buffer size of 50 images per stage, our method consistently outperforms competitors, even with ten times less storage. This adaptability underscores our method’s efficacy. These results attest to our method’s prowess in accurately approximating the forgery distribution and retaining knowledge adeptly, even in environments with pronounced domain gaps. Importantly, our method doesn’t just alleviate catastrophic forgetting but also matches the performance levels of contemporary forgery attacks (from the latest stage) seen in other methodologies.

Quantitative Results on Protocol 3. To rigorously assess our method’s performance across longer sequences, we executed comparative tests using the more complex Protocol 3. The sequence followed is **DF** \rightarrow **Celeb-DF1** \rightarrow **NT** \rightarrow **WildDeepfake1** \rightarrow **FS** \rightarrow **DFDC1** \rightarrow **F2F** \rightarrow **Celeb-DF2** \rightarrow **WildDeepfake2** \rightarrow **DFDC2** with ‘1’ and ‘2’ indicating separate portions of the original dataset. Results for both AVG and

Method	Buffer/ Stage	AVG		PRE	
		ACC	AUC	ACC	AUC
SFT	0	72.51	80.30	68.90	76.64
LwF	0	74.32	83.81	70.99	78.58
MAS	0	73.88	83.56	69.89	78.92
NCM	0	72.98	81.25	70.37	77.38
iCaRL	500	74.17	83.50	72.77	79.94
SCR	500	75.66	85.61	72.79	80.69
FReTAL	500	76.18	84.97	73.00	81.53
DER++	500	73.87	82.21	71.19	78.98
Co2L	500	75.66	84.43	72.95	81.43
HDP	0	<u>77.17</u>	<u>85.94</u>	<u>74.10</u>	<u>82.01</u>
HDP	50	80.15	87.97	75.47	83.82

Table 3: Quantitative results on protocol3. We evaluate the last model on the test sets of all tasks in terms of ACC and AUC. The buffer represents the memory bank budget save the previous images per stage. Underline indicate the sub-optimal results.

PRE, expressed in terms of ACC and AUC for Protocol 3, are detailed in Tab 3. Evidently, our method attains state-of-the-art (SOTA) results irrespective of buffer size usage. When pitted against non-buffer reliant strategies like LwF, HDP’s PRE outclasses by a 4% margin in ACC. We also tailored our HDP with a buffer size of 50 samples per stage, akin to our adaptation in Protocol 2. When juxtaposed with methods that utilize buffers of 500 samples, our strategy yields superior outcomes using just 50 samples at each stage. For instance, when gauging in

Method	Deepfakes		Face2Face		FaceSwap		NeuralTextures		AVG		PRE	
	ACC	AUC	ACC	AUC	ACC	AUC	ACC	AUC	ACC	AUC	ACC	AUC
EN-B4	76.88	91.88	68.57	85.57	59.74	72.78	95.53	98.43	75.07	87.16	67.29	88.36
EN-B4+HDP	93.10	98.17	91.90	96.86	93.47	97.52	94.81	97.12	93.32	97.41	94.94	98.50
F3-Net	80.94	93.04	69.71	82.70	63.55	74.03	94.55	97.89	77.18	86.91	69.33	89.57
F3-Net+HDP	91.65	96.26	89.06	94.70	90.99	96.15	94.21	97.97	91.49	96.22	93.51	97.77
MAT	77.13	92.30	67.75	83.33	66.75	73.49	95.20	98.54	76.81	86.90	71.96	90.72
MAT+HDP	92.55	97.14	90.76	95.26	94.23	97.94	95.23	98.07	93.13	96.84	94.36	98.65
SIA	78.52	93.68	71.29	87.21	61.15	75.03	95.44	98.40	76.60	88.58	72.39	91.28
SIA+HDP	92.33	98.01	91.11	95.59	93.01	97.31	95.47	97.39	92.98	97.07	95.30	97.58
UIA-VIT	81.43	93.57	70.77	83.51	61.05	71.23	95.98	98.25	77.30	86.64	70.33	90.55
UIA-VIT+HDP	93.22	97.52	89.78	95.21	95.07	98.01	95.22	97.99	93.32	97.18	94.81	98.99

Table 4: Quantitative results on protocol 1 on three SOTA face forgery detection models in terms of ACC and AUC. We evaluate the last model on all the previous test sets.

Eq.5	Eq.6	Eq.7	AVG		PRE	
			ACC	AUC	ACC	AUC
			75.07	87.16	67.29	88.36
✓			77.17	90.33	74.33	92.21
✓	✓		79.35	92.21	77.39	94.40
		✓	81.58	93.76	81.19	95.34
✓		✓	91.79	96.63	90.71	97.11
✓	✓	✓	93.32	97.41	94.94	98.50

Table 5: Ablation study on the influence of different components on protocol1 in terms of ACC and AUC.

terms of ACC, HDP surpasses FReTAL by 4% in AVG and 2% in PRE. These findings underline the potency of our proposed HDP in extended sequence environments, affirming its prospective utility in real-world applications.

Comparison with Existing Detection Methods. To underscore the versatility of HDP, we integrated it with three state-of-the-art (SOTA) face forgery detection methods: F3Net [Qian et al. \(2020\)](#), Multi-Attentional (MAT) [Zhao et al. \(2021a\)](#), SIA [Sun et al. \(2022\)](#), and UIA-VIT [Zhuang et al. \(2022\)](#). The results, presented in Tab. 4, show that while standalone SOTA methods deliver sub-optimal performance, their efficiency improves notably in terms of both AVG and PRE when combined with the HDP framework. Specifically, integrating HDP into MAT leads to a 23% improvement in the PRE metric (in terms of ACC), while F3-Net experiences an approximate 16% enhancement in AVG. These findings not only highlight the robustness of our method but also attest to its adaptability.

UAP Attack Rate	AVG		PRE	
	ACC	AUC	ACC	AUC
0.6	90.35	96.24	90.33	96.07
0.7	91.03	96.58	92.34	97.30
0.8	93.32	97.41	94.94	98.50
0.9	92.89	97.13	94.10	97.73
1.0	92.37	97.29	93.67	97.25

Table 6: Ablation study on UAP attack rate.

4.3 Ablation Study

Ablation study on components. The optimization process of our HDP considers three main equations: Eq.5 which targets the training of pseudo-forged samples, Eq.6 focusing on the distillation of pseudo-forged features, and Eq.7 for real feature distillation. An ablation study was conducted to understand the contributions of each of these equations to the model’s performance. The AVG and PRE metrics under Protocol1 in terms of ACC and AUC are shown in Tab. 6. Our observations are multifold: (1). When the regularization of the real distribution is absent, the model witnesses a marked performance decline. This can be attributed to the distribution of pseudo-forged samples, which tends to sway in tandem with shifts in the genuine distribution. This is evident upon contrasting the second, third, and fifth rows. (2). An analysis of the fourth row suggests that a constrained focus on real sample distillation yields sub-optimal results. Consequently, the model’s proficiency to accurately discern forgery distributions is compromised. (3). Notably, the model’s pinnacle of efficacy is attained when all three equations are concurrently and cohesively

Method	Buffer	Epoch	Total Time	AVG	PRE
SFT	0	20	2500s	75.07	67.29
LwF	0	20	2900s	77.63	74.09
MAS	0	20	3080s	80.43	83.76
NCM	0	20	3140s	75.53	69.13
iCaRL	500	20	3517s	83.57	82.82
SCR	500	20	3497s	80.69	75.29
FReTAL	500	20	4437s	89.53	80.07
DER++	500	20	4357s	79.12	80.80
Co2L	500	20	4557s	80.19	77.52
HDP	0	20	4096s	93.32	94.94
HDP	0	10	2136s	91.32	90.63

Table 7: Analysis of time consumption of each method. Total time represents time spent at each stage. The buffer represents the memory bank budget saved for the previous images per stage. We use ACC as the metric of AVG and PRE.

activated. This substantiates the inherent interdependence of these equations, underscoring the superior results borne from their synergy.

Ablation study on attack rate. The generated UAP can represent the discriminative feature of the training set, but there exist many out-of-distribution samples. Thus, the UAP Attack rate, which represents the proportion of successful attacks when generating UAP, is important in our method. To investigate the best attack rate, we conduct an ablation study on it and reported in Tab. 6. We varied the attack success rate within $[0.6, 0.7, 0.8, 0.9, 1.0]$, the best results were obtained when the attack rate is 0.8. Since there are some outliers in the training dataset, the attack rate cannot be set too high, otherwise it will cause overfitting. If the attack rate is lower than 0.8, the ability of UAP to represent the distribution will decrease, which will affect the simulation of the distribution and cause knowledge forgetting.

4.4 Experimental Analysis

Analysis of Time Consumption. To intuitively show the time and memory requirements of each comparison method, we detail the training epoch, memory bank size, and total time per stage alongside AVG and PRE metrics in terms of ACC. From the results in Tab. 7, it’s evident that our method delivers a commendable performance with a significantly reduced memory footprint and training time compared to recent methods like FReTAL, DER++, and Co2L, all of which require 20 training epochs. Moreover, when

we reduced our training epochs from 20 to 10, our proposed HDP method still managed to attain state-of-the-art performance, and in terms of time efficiency, it even surpassed SFT. These findings robustly underscore the efficiency and potency of our approach.

Analysis of Distribution Change. Our method intends to alleviate the catastrophic forgetting by rehearsing the simulated forgery distribution via UAP-based pseudo samples. To show the dynamic process of CFFD, we draw the feature distribution of baseline (SFT) and our method using t-SNE. Specifically, we visualize the four-step models *i.e.* Deepfakes, Face2Face, FaceSwap, and NeuralTextures of protocol1 with real, corresponding forgery, corresponding pseudo samples and previous forgery feature distributions, respectively. The results are shown in Fig. 4. We can observe that 1) for the SFT model, the overlap between previous forgery features and real features becomes more and more obvious with the increase of the attack, which demonstrates the phenomenon of catastrophic forgetting. 2) For our method, there exists an obvious decision boundary between the previous forgery feature and the real feature in every stage, which demonstrates the effectiveness of the anti-forgetting of our method. 3) The distribution of pseudo-forged features and actual forgery features is resembling and overlapping with each other. This phenomenon can support the motivation that uses these pseudo samples to simulate the forgery distribution.

5 Practicals of CFFD

As AIGC advances, the variety of manipulated faces increases, making it impossible for the detection model to acquire all types of training data at once. This results in poor performance of the model when confronted with unfamiliar domain data, which severely constrains the deployment of the detection model. Although some methods have been proposed to enhance the generalization of the model, even the SOTA generalization models are still far from practical application. For instance, on the Celeb-DF dataset, the best generalization method achieves an AUC of 84% under the cross-domain setting, while the intra-domain performance is 99% using the same backbone. Therefore, in real-world applications, the detection model should be updated along with the

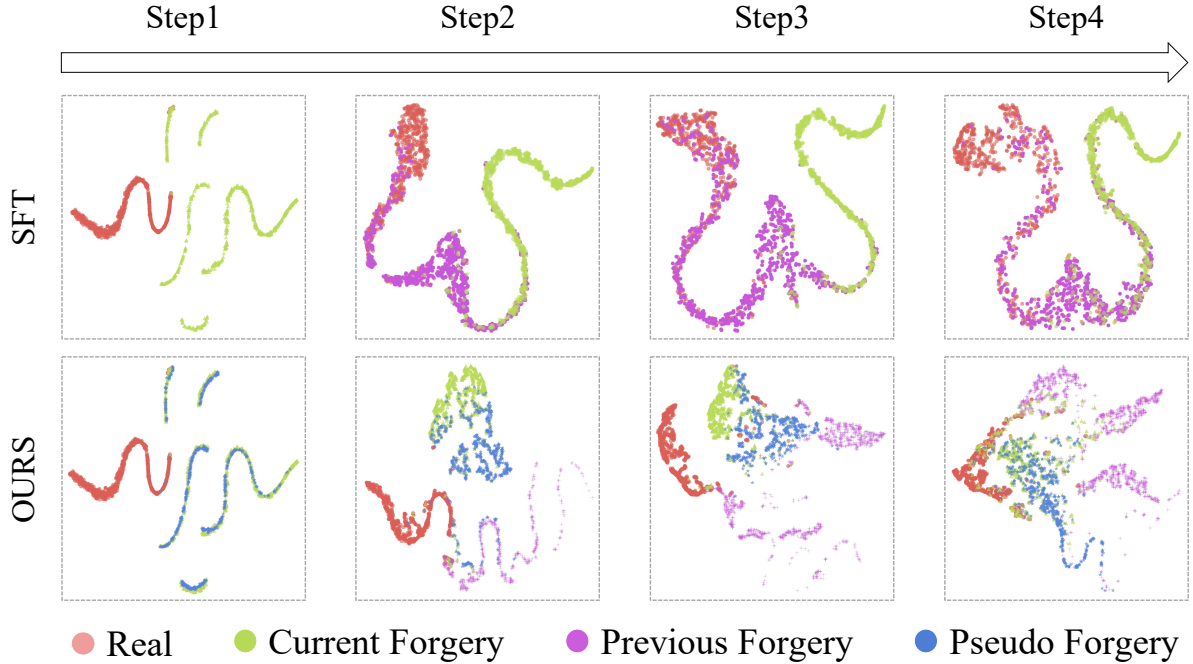


Fig. 4: Visualization of feature distribution on protocol1 via t-SNE. Step1 to step4 represents the Deepfakes, Face2Face, FaceSwap and NeuralTextures, respectively.

emergence of new forgery methods. A naive way to update the model is to combine the newly collected data and historical data for training, but this has two drawbacks: first, it will consume a lot of computational and storage resources; second, it will cause security issues such as data leakage. Therefore, in this paper, we focus on the problem of continual face forgery detection (CFFD), which aims to enable the model to learn new data and avoid forgetting the previous knowledge simultaneously. We believe that the setting of CFFD will contribute to the deployment and promotion of face forgery detection models.

6 Conclusion

In this work, we focus on a challenging and practical setting, named Continual Face Forgery face detection (CFFD), which enables efficient learning to deal with continually new attacks while mitigating catastrophic forgetting. Specifically, we propose a novel historical distribution preserving framework, which preserves the previous forgery distribution based on Universal Adversarial Perturbation (UAP), and the knowledge distillation is

further introduced to maintain distribution variation of real faces across models over different periods. Correspondingly, we also build a new benchmark for CFFD with three different evaluation protocols. Extensive experiments on the novel benchmarks demonstrate that our method outperforms other SOTA competitors at a lower storage cost. The results affirm the potential of our approach as a robust and efficient solution in the ongoing battle against face forgery and underline the significance of continual learning in cybersecurity.

7 Acknowledgments

This work was supported by National Key R&D Program of China (No.2022ZD0118202), the National Science Fund for Distinguished Young Scholars (No.62025603), the National Natural Science Foundation of China (No. U21B2037, No. U22B2051, No. 62176222, No. 62176223, No. 62176226, No. 62072386, No. 62072387, No. 62072389, No. 62002305 and No. 62272401), and the Natural Science Foundation of Fujian Province of China (No.2021J01002, No.2022J06001).

References

- Thies, J., Zollhöfer, M., Nießner, M., Valgaerts, L., Stamminger, M., Theobalt, C.: Real-time expression transfer for facial reenactment. *ACM Trans. Graph.* **34**(6), 183–1 (2015)
- Rossler, A., Cozzolino, D., Verdoliva, L., Riess, C., Thies, J., Nießner, M.: Faceforensics++: Learning to detect manipulated facial images. In: *ICCV*, pp. 1–11 (2019)
- Dolhansky, B., Bitton, J., Pflaum, B., Lu, J., Howes, R., Wang, M., Ferrer, C.C.: The deepfake detection challenge dataset. *arXiv preprint arXiv:2006.07397* (2020)
- Chen, S., Yao, T., Chen, Y., Ding, S., Li, J., Ji, R.: Local relation learning for face forgery detection. *AAAI* (2021)
- Qian, Y., Yin, G., Sheng, L., Chen, Z., Shao, J.: Thinking in frequency: Face forgery detection by mining frequency-aware clues. In: *ECCV*, pp. 86–103 (2020). Springer
- Dang, H., Liu, F., Stehouwer, J., Liu, X., Jain, A.K.: On the detection of digital face manipulation. In: *CVPR*, pp. 5781–5790 (2020)
- Afchar, D., Nozick, V., Yamagishi, J., Echizen, I.: Mesonet: a compact facial video forgery detection network. In: *WIFS*, pp. 1–7 (2018). IEEE
- Sun, K., Liu, H., Ye, Q., Liu, J., Gao, Y., Shao, L., Ji, R.: Domain general face forgery detection by learning to weight. In: *AAAI*, vol. 35, pp. 2638–2646 (2021)
- Luo, A., Kong, C., Huang, J., Hu, Y., Kang, X., Kot, A.C.: Beyond the prior forgery knowledge: Mining critical clues for general face forgery detection. *arXiv preprint arXiv:2304.12489* (2023)
- Luo, A., Li, E., Liu, Y., Kang, X., Wang, Z.J.: A capsule network based approach for detection of audio spoofing attacks. In: *ICASSP 2021-2021 IEEE International Conference on Acoustics, Speech and Signal Processing (ICASSP)*, pp. 6359–6363 (2021). IEEE
- Li, L., Bao, J., Zhang, T., Yang, H., Chen, D., Wen, F., Guo, B.: Face x-ray for more general face forgery detection. In: *CVPR*, pp. 5001–5010 (2020)
- Sun, K., Yao, T., Chen, S., Ding, S., Ji, R., *et al.*: Dual contrastive learning for general face forgery detection. In: *AAAI* (2022)
- Luo, Y., Zhang, Y., Yan, J., Liu, W.: Generalizing face forgery detection with high-frequency features. In: *CVPR*, pp. 16317–16326 (2021)
- Li, C., Huang, Z., Paudel, D.P., Wang, Y., Shahbazi, M., Hong, X., Van Gool, L.: A continual deepfake detection benchmark: Dataset, methods, and essentials. In: *Proceedings of the IEEE/CVF Winter Conference on Applications of Computer Vision*, pp. 1339–1349 (2023)
- Li, Z., Hoiem, D.: Learning without forgetting. *IEEE transactions on pattern analysis and machine intelligence* **40**(12), 2935–2947 (2017)
- Hou, S., Pan, X., Loy, C.C., Wang, Z., Lin, D.: Learning a unified classifier incrementally via rebalancing. In: *CVPR*, pp. 831–839 (2019)
- Kirkpatrick, J., Pascanu, R., Rabinowitz, N., Veness, J., Desjardins, G., Rusu, A.A., Milan, K., Quan, J., Ramalho, T., Grabska-Barwinska, A., *et al.*: Overcoming catastrophic forgetting in neural networks. *Proceedings of the national academy of sciences* **114**(13), 3521–3526 (2017)
- Rusu, A.A., Rabinowitz, N.C., Desjardins, G., Soyer, H., Kirkpatrick, J., Kavukcuoglu, K., Pascanu, R., Hadsell, R.: Progressive neural networks. *arXiv preprint arXiv:1606.04671* (2016)
- Xu, J., Zhu, Z.: Reinforced continual learning. *NeurIPS* **31** (2018)
- Verma, V.K., Liang, K.J., Mehta, N., Rai, P., Carin, L.: Efficient feature transformations for discriminative and generative continual learning. In: *CVPR*, pp. 13865–13875 (2021)
- Rebuffi, S.-A., Kolesnikov, A., Sperl, G., Lampert, C.H.: icarl: Incremental classifier and representation learning. In: *CVPR*, pp. 2001–2010 (2017)

- Aljundi, R., Lin, M., Goujaud, B., Bengio, Y.: Online continual learning with no task boundaries. arXiv preprint arXiv:1903.08671 (2019)
- Chaudhry, A., Gordo, A., Dokania, P.K., Torr, P., Lopez-Paz, D.: Using hindsight to anchor past knowledge in continual learning. arXiv preprint arXiv:2002.08165 **3** (2020)
- Jetley, S., Lord, N., Torr, P.: With friends like these, who needs adversaries? *NeurIPS* **31** (2018)
- Zhang, C., Benz, P., Imtiaz, T., Kweon, I.S.: Understanding adversarial examples from the mutual influence of images and perturbations. In: *CVPR*, pp. 14521–14530 (2020)
- Matern, F., Riess, C., Stamminger, M.: Exploiting visual artifacts to expose deepfakes and face manipulations. In: *WACVW*, pp. 83–92 (2019). IEEE
- Yang, X., Li, Y., Lyu, S.: Exposing deep fakes using inconsistent head poses. In: *ICASSP*, pp. 8261–8265 (2019). IEEE
- Stehouwer, J., Dang, H., Liu, F., Liu, X., Jain, A.: On the detection of digital face manipulation. arXiv preprint arXiv:1910.01717 (2019)
- Zhao, H., Zhou, W., Chen, D., Wei, T., Zhang, W., Yu, N.: Multi-attentional deepfake detection. *CVPR* (2021)
- Zhao, T., Xu, X., Xu, M., Ding, H., Xiong, Y., Xia, W.: Learning self-consistency for deepfake detection. In: *CVPR*, pp. 15023–15033 (2021)
- Delange, M., Aljundi, R., Masana, M., Parisot, S., Jia, X., Leonardis, A., Slabaugh, G., Tuytelaars, T.: A continual learning survey: Defying forgetting in classification tasks. *IEEE Transactions on Pattern Analysis and Machine Intelligence* (2021)
- Aljundi, R., Babiloni, F., Elhoseiny, M., Rohrbach, M., Tuytelaars, T.: Memory aware synapses: Learning what (not) to forget. In: *ECCV*, pp. 139–154 (2018)
- Wang, Z., Zhang, Z., Lee, C.-Y., Zhang, H., Sun, R., Ren, X., Su, G., Perot, V., Dy, J., Pfister, T.: Learning to prompt for continual learning. arXiv preprint arXiv:2112.08654 (2021)
- Buzzega, P., Boschini, M., Porrello, A., Abati, D., Calderara, S.: Dark experience for general continual learning: a strong, simple baseline. *NeurIPS* **33**, 15920–15930 (2020)
- Wu, Y., Chen, Y., Wang, L., Ye, Y., Liu, Z., Guo, Y., Fu, Y.: Large scale incremental learning. In: *CVPR*, pp. 374–382 (2019)
- Moosavi-Dezfooli, S.-M., Fawzi, A., Fawzi, O., Frossard, P.: Universal adversarial perturbations. In: *CVPR*, pp. 1765–1773 (2017)
- Szegedy, C., Zaremba, W., Sutskever, I., Bruna, J., Erhan, D., Goodfellow, I., Fergus, R.: Intriguing properties of neural networks. arXiv preprint arXiv:1312.6199 (2013)
- Moosavi-Dezfooli, S.-M., Fawzi, A., Frossard, P.: Deepfool: a simple and accurate method to fool deep neural networks. In: *CVPR*, pp. 2574–2582 (2016)
- Moosavi-Dezfooli, S.-M., Fawzi, A., Fawzi, O., Frossard, P., Soatto, S.: Robustness of classifiers to universal perturbations: A geometric perspective. *ICLR* (2018)
- Chaubey, A., Agrawal, N., Barnwal, K., Guliani, K.K., Mehta, P.: Universal adversarial perturbations: A survey. arXiv preprint arXiv:2005.08087 (2020)
- Li, Y., Yang, X., Sun, P., Qi, H., Lyu, S.: Celeb-df: A large-scale challenging dataset for deepfake forensics. In: *CVPR*, pp. 3207–3216 (2020)
- Zi, B., Chang, M., Chen, J., Ma, X., Jiang, Y.-G.: Wildeepfake: A challenging real-world dataset for deepfake detection. In: *ACM MM*, pp. 2382–2390 (2020)
- Tan, M., Le, Q.V.: Efficientnet: Rethinking model scaling for convolutional neural networks. *ICML* (2019)
- Deng, J., Dong, W., Socher, R., Li, L.-J., Li, K., Fei-Fei, L.: Imagenet: A large-scale hierarchical

- image database. In: CVPR, pp. 248–255 (2009).
Ieee
- Li, J., Wang, Y., Wang, C., Tai, Y., Qian, J., Yang, J., Wang, C., Li, J., Huang, F.: Dsf: dual shot face detector. In: CVPR, pp. 5060–5069 (2019)
- Mai, Z., Li, R., Kim, H., Sanner, S.: Supervised contrastive replay: Revisiting the nearest class mean classifier in online class-incremental continual learning. In: CVPR, pp. 3589–3599 (2021)
- Kim, M., Tariq, S., Woo, S.S.: Fretal: Generalizing deepfake detection using knowledge distillation and representation learning. In: CVPR, pp. 1001–1012 (2021)
- Yan, S., Xie, J., He, X.: Der: Dynamically expandable representation for class incremental learning. In: CVPR, pp. 3014–3023 (2021)
- Cha, H., Lee, J., Shin, J.: Co2l: Contrastive continual learning. In: ICCV, pp. 9516–9525 (2021)
- Sun, K., Liu, H., Yao, T., Sun, X., Chen, S., Ding, S., Ji, R.: An information theoretic approach for attention-driven face forgery detection. In: ECCV, pp. 111–127 (2022). Springer
- Zhuang, W., Chu, Q., Tan, Z., Liu, Q., Yuan, H., Miao, C., Luo, Z., Yu, N.: Uia-vit: Unsupervised inconsistency-aware method based on vision transformer for face forgery detection. In: European Conference on Computer Vision, pp. 391–407 (2022). Springer